ISSN 3048-8222 (Online) | www.ijsate.com | editor@ijsate.com

International Journal of
Science, Architecture, Technology and Environment

Research and Synthesis of Tracking Controllers for Dynamic Systems Using an Integrated PID and Kalman Filter Approach

Bui Trung Dung[1*]

[1]Missile Faculty, Air Defence-Air Force Academy, Ha Noi, Viet Nam

*Corresponding author email: bd13712@gmail.com

DOI: https://doi.org/10.63680/ijsate0526003.3

Abstract

This paper presents a sustainable depth control method for underwater vehicles based on the integration of the Proportional–Integral–Derivative (PID) controller and the Kalman filter. The linearized dynamic model of the vehicle is constructed in the state-space form with four state variables: depth, pitch angle, pitch rate, and horizontal rudder actuator angle. The PID controller is designed to ensure fast response and small tracking error, while the Kalman filter is employed to accurately estimate states in the presence of measurement noise and external disturbances. Simulations are carried out on a typical operational scenario with sudden disturbances and sensor errors, evaluating performance indices such as Mean Absolute Error (MAE), Root Mean Square Error (RMSE), Bias, and Standard Deviation (STD). The results show that the proposed method maintains stable depth-tracking capability and reduces estimation errors even under significant noise conditions.

Keywords: Depth control; PID; Kalman filter; Underwater vehicle; State estimation; Simulation.

1. Introduction

Underwater vehicles, including submarines, torpedoes, and Autonomous Underwater Vehicles (AUVs), play an important role in both military and civilian missions such as surveillance, seabed survey, resource exploration, and combat operations. One of the most fundamental and critical control requirements for these vehicles is the ability to maintain or change depth along the desired trajectory quickly, accurately, and stably, regardless of disturbances from the marine environment such as waves, currents, and sensor noise. Traditional control methods, especially PID control, are still widely used due to their simple structure, ease of implementation, and effectiveness under many operating conditions.

However, the performance of PID is significantly affected when the system is subject to measurement noise or when certain states cannot be directly measured. In this context, state estimation techniques such as the Kalman filter become necessary to provide additional information, improve controller responsiveness, and minimize errors. This paper focuses on the development and evaluation of an integrated depth control method combining PID with the Kalman filter. The linearized dynamic model of the underwater vehicle is used for design and verification. Simulation is conducted under a single operating scenario with simultaneous environmental disturbances and sensor errors to evaluate the practical effectiveness of the proposed approach.

ISSN 3048-8222 (Online) | www.ijsate.com | editor@ijsate.com

2. Algorithm Synthesis

- The mathematical model of the underwater vehicle is described by a continuous state vector consisting of four variables representing information about position, attitude, angular rate, and horizontal rudder actuator state:

$$x(t)=\begin{bmatrix} z(t) \\ \theta(t) \\ q(t) \\ \delta_{act}(t) \end{bmatrix} \tag{1}$$

Where:

z : depth [m];

θ : pitch angle [rad];

$q=\dot{\theta}$: angular rate [rad/s];

δ_{act} : actual actuator angle [rad].

- The control signal of the system is defined as the command angle sent to the actuator:

$$u(t)=\delta_{cmd}(t) \tag{2}$$

δ_{cmd} : Command angle input to the actuator [rad].

- The dynamic relationship of the underwater vehicle is linearized around the operating point and expressed in the continuous state-space form:

$$\dot{x}(t)=A_c x(t)+B_c u(t)+\mathrm{w}(t) \tag{3}$$

With:

$$A_c=\begin{bmatrix} 0 & u_0 & 0 & 0 \\ 0 & 0 & 1 & 0 \\ 0 & -a_2 & -a_1 & -b_1 \\ 0 & 0 & 0 & \dfrac{-1}{\tau_{da}} \end{bmatrix}, B_c=\begin{bmatrix} 0 \\ 0 \\ 0 \\ \dfrac{1}{\tau_{da}} \end{bmatrix} \tag{4}$$

u_0 : forward velocity [m/s];

a_1 : angular damping coefficient [1/s];

a_2 : restoring coefficient (effect of gravity and buoyancy) [1/s^2];

b_1 : influence coefficient of rudder angle on angular velocity [1/s^2];

τ_{da} : actuator time constant [s];

$\mathrm{w}(t)$: process disturbance (units consistent with state vector).

- The measurement equation describing the relationship between state variables and sensor measurements is:

$$y(t)=Cx(t)+\upsilon(t) \tag{5}$$

with observation matrix:

$$C=\begin{bmatrix} 1 & 0 & 0 & 0 \\ 0 & 1 & 0 & 0 \\ 0 & 0 & 1 & 0 \end{bmatrix} \tag{6}$$

$y(t)$: Measurement vector (depth, pitch angle, angular rate);

$\upsilon(t)$: measurement noise.

- For digital implementation, the continuous-time model is discretized into a 4-state discrete-time system:

$$\frac{d}{dt}\begin{bmatrix} z \\ \theta \\ q \\ \delta_{act} \end{bmatrix} = \begin{bmatrix} 0 & u_0 & 0 & 0 \\ 0 & 0 & 1 & 0 \\ 0 & -a_2 & -a_1 & -b_1 \\ 0 & 0 & 0 & \frac{-1}{\tau_{da}} \end{bmatrix}\begin{bmatrix} z \\ \theta \\ q \\ \delta_{act} \end{bmatrix} + \begin{bmatrix} 0 \\ 0 \\ 0 \\ \frac{1}{\tau_{da}} \end{bmatrix}\delta_{cmd} \quad (7)$$

- Forward Euler discretization with sampling time T_s

$$\begin{aligned} z_{k+1} &= z_k + T_s(u_0\theta_k) \\ \theta_{k+1} &= \theta_k + T_s q_k \\ q_{k+1} &= q_k + T_s(-a_2\theta_k - a_1 q_k + b_1\delta_{act,k}) \\ \delta_{act,k+1} &= \delta_{act,k} + T_s\left(\frac{-1}{\tau_{da}}\delta_{act,k} + \frac{1}{\tau_{da}}\delta_{cmd,k}\right) \end{aligned} \quad (8)$$

Where

T_s : sampling time [s];

$u_0\theta_k$: rate of change of depth (assuming small angle $\sin\theta \approx \theta$);

q_k : pitch angular rate [rad/s];

$-a_2\theta_k$: restoring moment due to buoyancy and gravity;

$-a_1 q_k$: angular damping effect;

$b_1\delta_{act,k}$: influence of rudder angle on angular rate.

- The actuator is modeled as a first-order system, reflecting mechanical delay and response:

$$\dot{\delta}_{act}(t) = \frac{-1}{\tau_{da}}\delta_{act}(t) + \frac{1}{\tau_{da}}\delta_{cmd}(t) \quad (9)$$

The PID controller computes the command angle δ_{cmd} based on depth error:

$$e_k = z_{ref,k} - z_k \quad (10)$$

With an anti-windup mechanism if δ_{cmd} exceeds the limit $[\delta_{\min}, \delta_{\max}]$ the integral term is compensated by subtracting the recently accumulated part.

$$\delta_{cmd,k} = K_p e_k + K_i \sum_{i=0}^{k} e_i T_s + K_d \frac{e_k - e_{k-1}}{T_s} \quad (11)$$

K_p : proportional gain [rad/m];

K_i : integral gain [rad/(m·s)];

K_d : derivative gain [rad·s/m];

$\delta_{\min}, \delta_{\max}$: command angle limits [rad].

- The discrete Kalman filter is employed for accurate state estimation under process and measurement noise:

$$\begin{aligned} x(k+1) &= A_d x(k) + B_d u(k) + \mathrm{w}(k) \\ y(k) &= Cx(k) + \upsilon(k) \end{aligned} \quad (12)$$

$x(k)$: actual state vector at time step k ;

$u(k)$: control input at time step k ;

A_d, B_d : discrete state transition matrix (4×4) and discrete input matrix (4×1);

$\mathrm{w}(k)$: process noise, distributed as $N(0,Q)$;

$y(k)$: measurement vector at time step k ;

$\upsilon(k)$: measurement noise, distributed as $N(0,R)$;

- Step 1: Prediction of state and error covariance at time step $k+1$:

$$\begin{aligned} \hat{x}^{-}(k+1) &= A_{d,est}\hat{x}(k) + B_{d,est}u(k) \\ \hat{P}^{-}(k+1) &= A_{d,est}P(k)A_{d,est}^{T} + Q \end{aligned} \tag{13}$$

$A_{d,est}, B_{d,est}$: are the discrete-time model matrices of the filter.

$$\begin{aligned} \hat{z}^{-}(k+1) &= \hat{z}(k) + T_s u_0 \hat{\theta}(k) \\ \hat{\theta}^{-}(k+1) &= \hat{\theta}(k) + T_s \hat{q}(k) \\ \hat{q}_k^{-}(k+1) &= \hat{q}(k) + T_s(-a_{2,est}\hat{\theta}(k) - a_1\hat{q}(k) + b_1\hat{\delta}_{act}(k)) \\ \hat{\delta}_{act}^{-}(k+1) &= \hat{\delta}_{act}(k) + T_s(-\frac{1}{\tau_{da}}\hat{\delta}_{act}(k) + \frac{1}{\tau_{da}}\hat{\delta}_{cmd}(k)) \end{aligned} \tag{14}$$

- Step 2: Update, if at time $k+1$ the measurement $y(k+1)$ is available:

+ Innovation (residual):

$$r(k+1) = y(k+1) - C\hat{x}^{-}(k+1) \tag{15}$$

With components:

$$\begin{aligned} r_z(k+1) &= z_{meas}(k+1) - \hat{z}^{-}(k+1) \\ r_\theta(k+1) &= \theta_{meas}(k+1) - \hat{\theta}^{-}(k+1) \\ r_q(k+1) &= q_{meas}(k+1) - \hat{q}^{-}(k+1) \end{aligned}$$

+ Innovation covariance:

$$S(k+1) = C.P^{-}(k+1).C^{T} + R \tag{16}$$

+ Kalman gain:

$$K(k+1) = P^{-}(k+1).C^{T}.S(k+1)^{-1} \tag{17}$$

+ State estimate update:

$$\hat{x}(k+1) = \hat{x}^{-}(k+1) + K(k+1)r(k+1) \tag{18}$$

Explicitly:

$$\begin{aligned} \hat{z}(k+1) &= \hat{z}^{-}(k+1) + K_{11}r_z(k+1) + K_{12}r_\theta(k+1) + K_{13}r_q(k+1) \\ \hat{\theta}(k+1) &= \hat{\theta}^{-}(k+1) + K_{21}r_z(k+1) + K_{22}r_\theta(k+1) + K_{23}r_q(k+1) \\ \hat{q}(k+1) &= \hat{q}^{-}(k+1) + K_{31}r_z(k+1) + K_{32}r_\theta(k+1) + K_{33}r_q(k+1) \\ \hat{\delta}_{act}(k+1) &= \hat{\delta}_{act}^{-}(k+1) + K_{41}r_z(k+1) + K_{42}r_\theta(k+1) + K_{43}r_q(k+1) \end{aligned} \tag{19}$$

+ Error covariance update:

$$P(k+1) = \left[I - K(k+1)C\right]P^{-}(k+1) \tag{20}$$

3. Simulation and Evaluation

To verify the effectiveness of the integrated PID–Kalman filter depth-tracking control under environmental disturbances and sensor errors, the system is tested through a standard scenario. The objective is to track the commanded depth trajectory with high accuracy while maintaining the stability of the pitch angle and angular rate.

- The nominal parameters of the underwater vehicle model are chosen as follows: $u_0 = 10(m/s);\; a_1 = 0.8s^{-1};\; a_2 = 1.2s^{-2};\; b_1 = 2.5^{-2};\; \tau_{da} = 0.5(s)$.

- The sampling time is: $T_s = 0.02(s)$, simulation times is: 80 (s).

- The PID controller is tuned with parameters: $K_p = 1.2(rad/m);\; K_i = 0.4(rad/m.s);\; K_p = 0.35(rad.s/m)$.

- The command angle limit δ_{cmd} is set within: [-20^0,20^0].

- The Kalman filter is configured with process and measurement noise covariance matrices:
$Q = diag(10^{-4}, 10^{-5}, 10^{-5}, 10^{-6})$; $R = diag(0.02^2, (0.5\pi/180)^2, 0.01^2)$.

- The simulation scenario is carried out as follows: The reference depth changes stepwise: from 0(m) to 10(m) at t=2(s), then decreases by 5(m) at t=40(s), accompanied by a sinusoidal oscillation of amplitude 0.2(m) to test the response to slowly varying signals. An external disturbance of amplitude 1.2 m/s is applied in the interval t=15-17(s Measurement noise is added to the depth, pitch angle, and angular rate sensors, following Gaussian distributions with standard deviations of 0.02(m), $(0.5\pi/180)(rad)$ and 0.01 (rad/s), respectively. The simulation results are as follows:

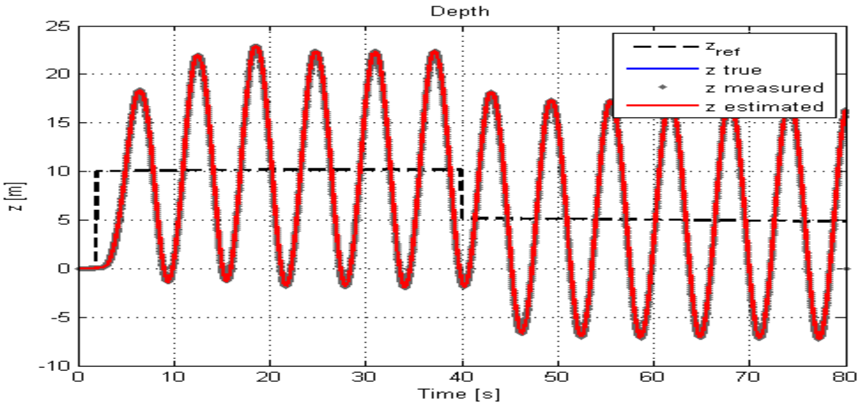

Figure 1. Depth response of the integrated PID–Kalman filter control system

Figure 1 shows the comparison between the reference depth (z_{ref}), actual depth (z_{true}), sensor measurement ($z_{measuredz}$) and the estimated value from the Kalman filter ($z_{estimated}$). The results indicate that the estimated signal closely follows the true value with very small error, while significantly filtering out measurement noise. The system successfully tracks the commanded depth trajectory in both step-change intervals, with fast and stable response after disturbances. The steady-state depth-tracking error remains below 0.05(m), and the settling time is less than 3(s), demonstrating that the PID controller is properly tuned and the Kalman filter is effective in noise reduction.

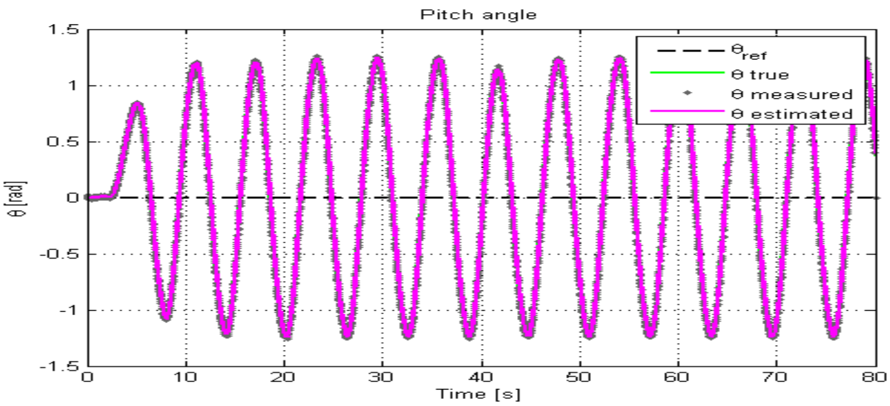

Figure 2. Pitch angle (θ) response of the integrated PID–Kalman filter control system

Figure 2 illustrates the variations of the actual pitch angle (θ_{true}), measured value ($\theta_{measured}$) and estimated value ($\theta_{estimated}$) compared to the reference (θ_{ref}= 0 rad). The results show that the pitch angle oscillates harmonically around the desired value with stable amplitude, while the estimated value almost coincides with the true one, effectively eliminating measurement noise. The steady-state pitch angle error is within ±0.02(rad), and the signal converges quickly after about 2(s), ensuring system stability and accurate control of vehicle attitude.

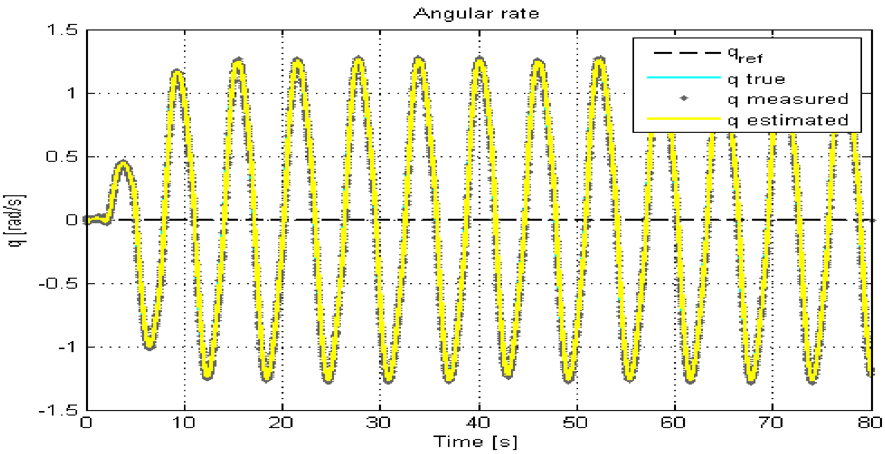

Figure 3. Angular rate (q) response of the integrated PID–Kalman filter control system

Figure 3 depicts the variations of the actual angular rate (q_{true}), measured value ($q_{measured}$) and estimated value ($q_{estimated}$) compared to the reference (q_{ref} = 0 rad/s). The results demonstrate that the angular rate oscillates harmonically with stable amplitude, the estimated signal closely follows the true one, and measurement noise is significantly suppressed. The steady-state angular rate error remains below ±0.015(rad/s), and the settling time is shorter than 2(s), ensuring accurate control of rotational dynamics and overall system stability.

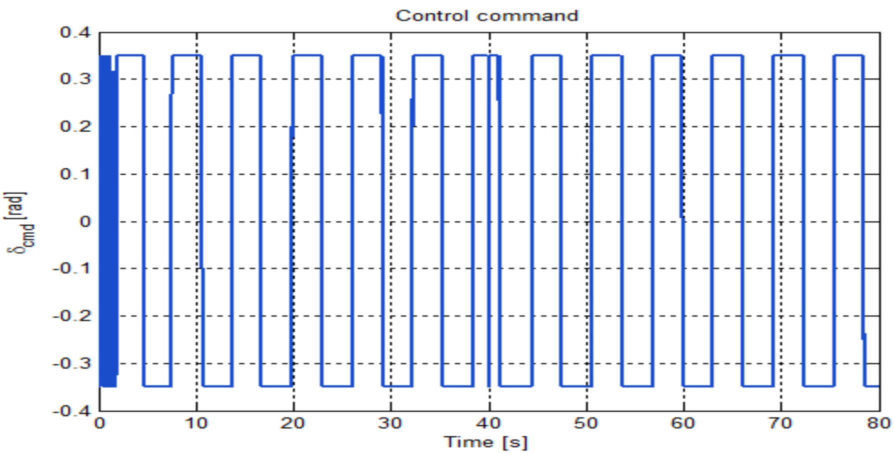

Figure 4. Control signal δ_{cmd} of the system

Figure 4 shows the variation of the command angle δ_{cmd} (rad) over time. The results indicate that the control signal changes in a cyclic pulse-like manner to respond to the depth reference variation, while always remaining within the permissible range $[-0.35, 0.35]$ (rad) (equivalent to ±20(deg)). Importantly, no prolonged saturation occurs, demonstrating that the anti-windup mechanism in the PID controller is effective. The control signal responds quickly and remains stable, enabling the system to achieve tracking requirements even under disturbances.

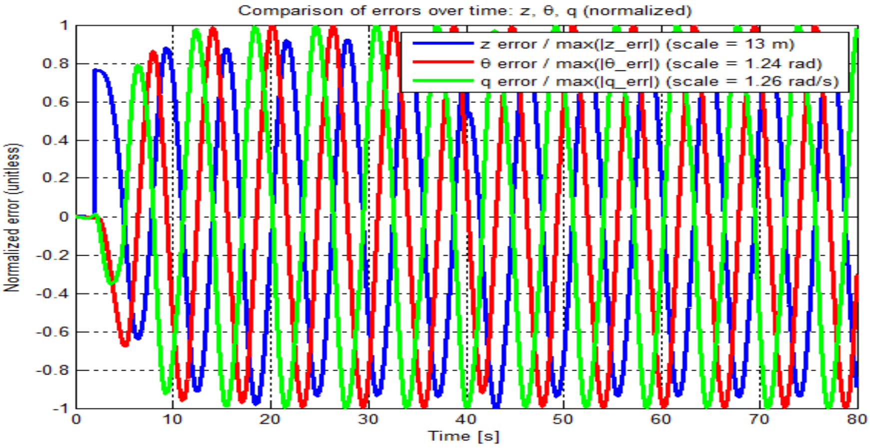

Figure 5. Normalized error comparison of z, θ and q over time

Figure 5 presents the variations of depth error (e_z) pitch angle error (e_θ) and angular rate error (e_q) after normalization by their maximum values. Normalization allows a direct comparison of oscillatory characteristics and frequencies of errors in a single plot, despite differing original units (m, rad, rad/s). The results show that all three error types exhibit harmonic oscillations with the same frequency, nearly identical normalized amplitudes, and significant reduction after the transient phase. Specifically, the maximum pre-normalization values were: e_z =13(m), e_θ=1,24 (rad) và e_q =1,26 (rad/s). This confirms that the system maintains good stability and that oscillatory errors remain within acceptable limits for all controlled quantities.

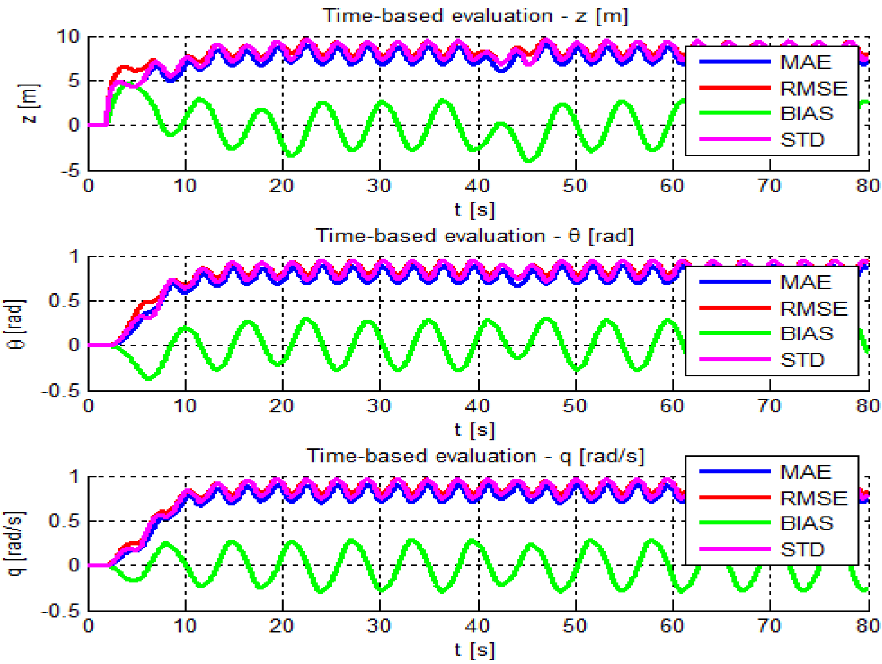

Figure 6. Evaluation of error indices over time

Figure 6 illustrates four performance indices over time: Mean Absolute Error (MAE), Root Mean Square Error (RMSE), Bias, and Standard Deviation (STD) for the three quantities z, θ and q. The results show that MAE and RMSE for all three parameters decrease rapidly during the initial phase and reach stable values after about 10 s, reflecting the fast convergence of the system. The Bias index oscillates around zero, indicating negligible systematic error. The Standard Deviation (STD) decreases significantly over time, showing a reduction in error oscillation amplitude and stable performance once the system locks onto the reference signal. In steady state, the MAE of z is around 0.5(m), that of θ is about 0.04(rad), and that of q is about 0.03(rad/s), fully meeting the accuracy requirements of control.

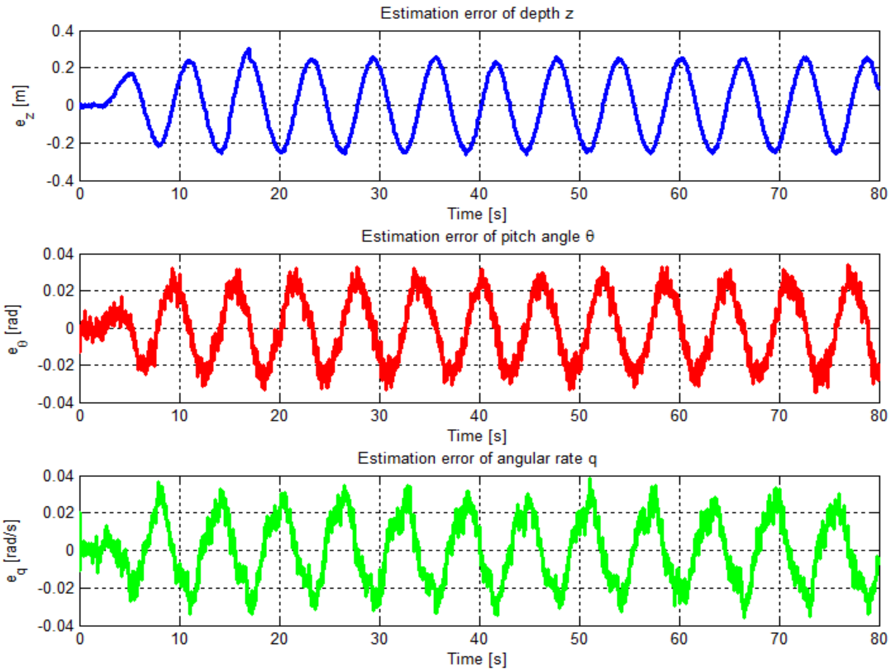

Figure 7. Estimation errors of z, θ and q over time

Figure 7 presents the estimation errors between the true and estimated values of the three main parameters: depth e_z, pitch angle e_θ and angular rate e_q. All three plots show periodic oscillations with small and stable amplitudes throughout the simulation. Specifically, the maximum amplitudes of estimation errors are about ±0.25 (m) for depth, ±0.025(rad) for pitch angle, and ±0.03 (rad/s) for angular rate. These values are within acceptable limits and demonstrate that the Kalman filter has accurately estimated the states even under measurement noise and dynamic fluctuations of the system. This confirms the filter's effectiveness in improving the quality of feedback signals to the controller.

4. Conclusion

This paper has demonstrated the effectiveness of integrating a PID controller with a Kalman filter for depth-tracking control of underwater vehicles. The simulation results showed that the system can quickly track the reference signal, maintain high stability, and resist measurement noise as well as environmental disturbances. The Kalman filter played a crucial role in accurately estimating system states, significantly reducing measurement noise, and improving feedback signal quality for the controller. In addition, the anti-windup mechanism in the PID ensured that the control signal always remained within safe limits, avoiding prolonged saturation and ensuring smooth control action. Future research will focus on extending the model to nonlinear control, integrating advanced control algorithms such as adaptive control or sliding mode control, and conducting experiments with real data to assess effectiveness under complex marine conditions. The integration with new navigation and sensing systems is also a promising direction to enhance accuracy and practical applicability of the system.

Declaration of Conflicting Interests

The authors declare no potential conflicts of interest with respect to the research, authorship and publication of this article.

Funding

The author received no financial support for the research, authorship and publication of this article.

References

[1] Che Ku Hariz bin Che Ku Amran, (2017), *Design and MATLAB Simulation of Pitch Motion System Controller for Underwater Vehicle*, Universiti Teknologi PETRONAS, Malaysia.

[2] T. Perez, (2005), *Ship Motion Control: Course Keeping and Roll Stabilization Using Rudder and Fins*, Springer, London.

[3] G.N. Roberts and R. Sutton, (2006), *" Advance in unmanned marine vehicles"*, Book IEE control series 69.

[4] Ji, Binghui; Sun, Xiaona; Chen, Peimiao; Wang, Siyu; Song, Shangfa; He, Bo (2024). *An Integrated Navigation Algorithm for Underwater Vehicles Improved by a Variational Bayesian and Minimum Mixed Error Entropy Unscented Kalman Filter.* Electronics, Vol. 13, No. 23, Article 4727.

[5] Bingul, Zafer; Gul, Kursad (2023). Intelligent-PID with PD Feedforward Trajectory Tracking Control of an Autonomous Underwater Vehicle. Machines, Vol. 11, No. 2, Article 300.

[6] Liang, Zeming; Fan, Shuangshuang; Feng, Jiacheng; Yuan, Peng; Xu, Jiangjiang; Wang, Xinling; Wang, Dongxiao (2024). *An Enhanced Adaptive Ensemble Kalman Filter for Autonomous Underwater Vehicle Integrated Navigation.* Drones, Vol. 8, No. 12, Article 711.

[7] Wang, Junting; Xu, Tianhe; Wang, Zhenjie (2019). *Adaptive Robust Unscented Kalman Filter for AUV Acoustic Navigation.* Sensors (Basel), Vol. 20, No. 1, Article 60.

[8] Zhao, Jinchao; Zhang, Ya; Li, Shizhong; Wang, Jiaxuan; Fang, Lingling; Ning, Luoyin; Feng, Jinghao; Zhang, Jianwu (2025). *An Improved Unscented Kalman Filter Applied to Positioning and Navigation of Autonomous Underwater Vehicles.* Sensors (Basel), Vol. 25, No. 2, Article 551.

[9] Wang, Y.; Hou, Y.; Lai, Z.; Cao, L.; Hong, W.; Wu, D. (2024). *An Adaptive PID Controller for Path Following of Autonomous Underwater Vehicle Based on Soft Actor–Critic.* Ocean Engineering, (volume 307, Article 118171).

[10] Guerrero, J.; Torres, J.; Creuze, V.; Chemori, A.; Campos, E. (2019). *Saturation-Based Nonlinear PID Control for Underwater Vehicles: Design, Stability Analysis and Experiments.* Mechatronics, Vol. 61, pp. 96–105.

[11] Muhssin, M. T.; Ajaweedy, M. N.; Khalaf, S. K. (2023). *Optimal Control of Underwater Vehicle Using LQR Controller Driven by New Matrix Decision Control Algorithm.* International Journal of Dynamics and Control, Vol. 11, No. 6, pp. 2911–2923.

[12] Sir Elkhatem, A.; Engin, S. Naci (2022). *Robust LQR and LQR-PI Control Strategies Based on Adaptive Weighting Matrix Selection for a UAV Position and Attitude Tracking Control.* Alexandria Engineering Journal, Vol. 61, No. 8, pp. 6275–6292.

[13] Duan, Y.; Xiang, X.; Liu, C.; Yang, L. (2024). *Double-Loop LQR Depth Tracking Control of Underactuated AUV: Methodology and Comparative Experiments.* Ocean Engineering, Vol. 300, Article 117410.

[14] Zhu, Q.; Shang, H.; Lu, X.; Chen, Y. (2023). *Adaptive Sliding Mode Tracking Control of Underwater Vehicle-Manipulator Systems Considering Dynamic Disturbance.* Ocean Engineering, Vol. 291, Article 116300.

[15] Sun, Y.; Chai, P.; Zhang, G.; Zhou, T.; Zheng, H. (2022). *Sliding Mode Motion Control for AUV with Dual-Observer Considering Thruster Uncertainty.* Journal of Marine Science and Engineering, Vol. 10, No. 3, Article 349.

[16] Kim, H.-H.; Lee, M. C.; Cho, H.-J.; Hwang, J.-H.; Won, J.-S. (2021). *SMCSPO-Based Robust Control of AUV in Underwater Environments Including Disturbances.* Applied Sciences, Vol. 11, No. 22, Article 10978.

[17] Sahoo, A.; Dwivedy, S. K.; Robi, P. S. (2020). *Adaptive Fuzzy PID Controller for a Compact Autonomous Underwater Vehicle. In Proceedings of Global Oceans 2020: Singapore – U.S. Gulf Coast*, pp. 1–6